Scientific paper

Possibility of C_{38} and $Si_{19}Ge_{19}$ Nanocages in Anode of Metal Ion Batteries: Computational Examination

Rong-Jun Bie,[1] Muhammad Kamran Siddiqui,[2] Razieh Razavi,[3,*] Milad Taherkhani[4] and Meysam Najafi[5,*]

[1] *School of Mathematics and Physics, Anhui Jianzhu University, Hefei 230601, China*

[2] *Department of Mathematics, Comsats Institute of Information Technology Sahiwal, Pakistan*

[3] *Department of Chemistry, Faculty of Science, University of Jiroft, Jiroft, Iran*

[4] *Department of Chemical Engineering, Amirkabir University of Technology (Tehran Polytechnic), Tehran, Iran*

[5] *Medical Biology Research Center, Kermanshah University of Medical Sciences, Kermanshah 67149-67346, Iran*

** Corresponding author: E-mail: R.Razavi@ujiroft.ac.ir and meysamnajafi2016@gmail.com Phone: +98-8337243181 Fax: +98-8337243181*

Received: 18-10-2017

Abstract

In this study, the potential of C_{38} and $Si_{19}Ge_{19}$ as anode electrodes of Li-ion, Na-ion and K-ion batteries via density functional theory was investigated. Obtained results showed that $Si_{19}Ge_{19}$ as anode electrode in metal-ion batteries has higher potential than C_{38} ca 0.18 V. Calculated results illustrated that K-ion battery has higher cell voltage and higher performance than Li-ion and Na-ion batteries ca 0.15 and 0.31 V, respectively. Results showed that halogen adoption increased the cell voltage of studied metal-ion batteries ca 1.5–2.2 V. Results show that, V_{cell} values of studied metal-ion batteries in water are higher than gas phase ca 0.46 V. Finally it can be concluded that F-doped $Si_{18}Ge_{19}$ as anode electrode in K-ion battery has the highest performance and it can be proposed as novel metal-ion batteries with high performance.

Keywords: Battery; nanocage; adoption; voltage; anode and halogen

1. Introduction

A rechargeable battery is a kind of electronic battery that has many electro-chemical various cells and it can be recharged several times. The cost of buying the rechargeable cells are higher than disposable cells, though rechargeable cells have lower destructive effects on environment. The rechargeable batteries have been used in starter of car, consumer devices and battery reservoir center.[1–6]

In lithium-ion battery (LIB) there are two processes; in charging process the lithium ions transferred from the positive to negative electrode and in discharge process the motion of lithium ions is the reverse of charge process. LIBs have high energy compression, high storage capacity, small memory effect and small self-evacuation.[7–12] The LIBs are expensive at actual, and a leakage of Lithium employed in LIBs can convert to an important issue in future.[13–18] The novel metal-ion batteries as the electrical storage batteries must have high capacity, high performance and high rate in charge and discharge processes.[18–23] The graphite due to low cost, cyclic durability, high energy stability has been used for anode electrode. In previous works, potential of some compounds such as germanium, transition metals and silicon for anode electrode have been examined.[24–33] In previous works the potential and capacities of nanoelectrods have been investigated and obtained results shown that nanotubes and nanocages have higher valences and energy capacitor than the graphite.[34–44] In previous studies, results confirmed that hydrogenation, adoption and functionalization of nanostructures improved their performances as anode materials in metal-ion batteries.[45–52] Due to positive effects of hydrogenation, adoption and functionalization of nanostructures on potentials of metal-ion batteries, many works have been done on usage of nanostructures as anode electrodes in metal-ion batteries.[52–55]

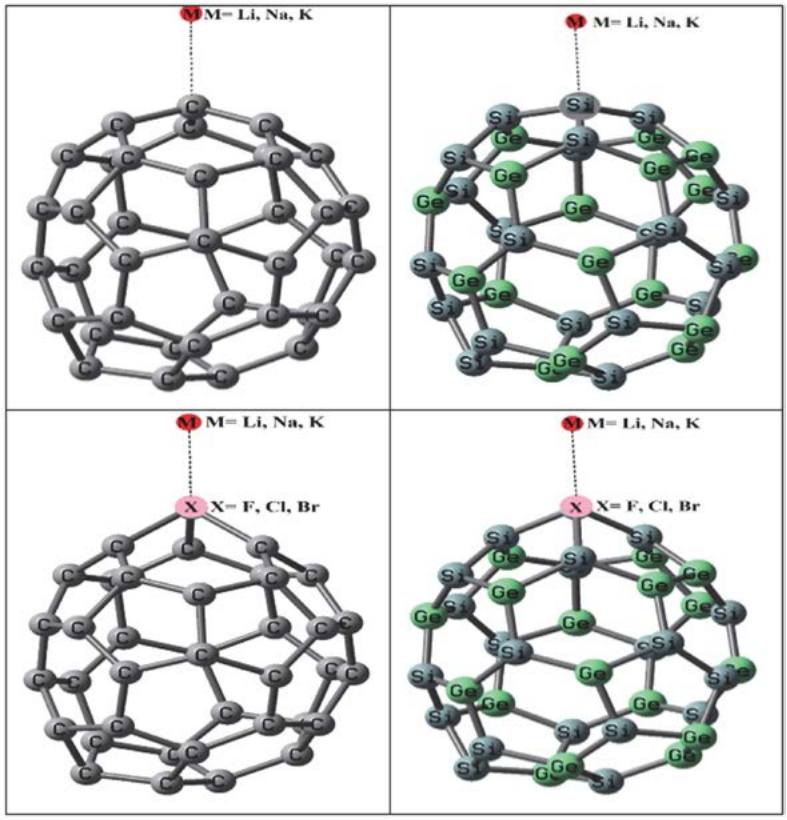

Figure 1. Structures of studied complexes.

In this study, in first step; the potential of C_{38} and $Si_{19}Ge_{19}$ nanocages as anode electrode in Li-ion battery via density functional theory was investigated. In second step; the C_{38} and $Si_{19}Ge_{19}$ nanocages doped with halogen atoms and effects of these adoptions on ability of Li-ion battery were examined. In third step; the potential of sodium-ion battery (NIB) and potassium-ion battery (KIB) were compared with Li-ion battery. In fourth step; the effects of halogen adoption on potential of studied NIBs and KIBs were investigated. In fifth step; novel metal-ion battery with high performance to use in industry will be proposed.

The main questions have been answered in this work are: (1) How much dose cell voltages of LIBs C_{38} and $Si_{19}Ge_{19}$ as anode electrodes? (2) Can NIBs and KIBs be suitable batteries with high performance? (3) Can halogen adoption increase the cell voltage of LIBs? (4) Which metal-ion batteries have high performance?

2. Computational Details

In this study, the geometries of C_{38} and $Si_{19}Ge_{19}$ were optimized via GAMESS software via DFT/ M06-2X theory and 6-311+G (2d, 2p) basis set. The adsorption of C_{38} and $Si_{19}Ge_{19}$ with halogen atoms (X = F, Cl, Br) were investigated and geometries of X-C_{38} and X-$Si_{19}Ge_{19}$ complexes were optimized at mentioned level of computational.

In this study the vibrational frequency calculations of all studied via DFT/M06-2X theory and 6-311+G (2d, 2p) basis set were done in order to evidence that all of the optimized geometries are factual local minima and also thermodynamic parameters of studied reactions were calculated by using of vibrational frequency analysis.[56–58]

The Gibbs free energy of process of adsorption of halogen atom (X = F, Cl, Br) on studied nanostructures were calculated via: G_{ad} = G (X-nanostructure) – G (nanostructure) – 0.5 G (X_2), where X-nanostructure corresponds to the Gibbs free energy of complexes of nanostructure with halogen atom, G (X_2) is the Gibbs free energy of the halogen molecule and G (nanostructure) is the Gibbs free energy of the nanostructure.[59–61]

The Gibbs free energy of adsorption of metal on nanostructure surfaces were calculated via: G_{ad} = G (M-nanostructure) – G (nanostructure) – G (M); where G (M-nanostructure) corresponds to the Gibbs free energy of complexes of nanostructure with metal and G (M) is the Gibbs free energy of the metal and G (nanostructure) is Gibbs free energy of the nanostructure.[62–64]

In this study, the energies of the basis set superposition error (E_{BSSE}) for studied interactions between nanostructures and metals were calculated by using of counterpoise correction method and obtained results showed that E_{BSSE} values are ca 0.05 Kcal/mol.

The energy difference between the highest occupied molecular orbital (HOMO) and the lowest unoccupied molecular orbital (LUMO) of studied nanostructures defined as HOMO–LUMO Gap (E_{HLG}) and it calculated via ($E_{HLG} = E_{LUMO} - E_{HOMO}$); where E_{LUMO} and E_{HOMO} are energies of LUMO and HOMO of studied nanostructures.[65–67]

In the cathode and anode of LIBs, NIBs and KIBs with hypothetical nanostructure anode it can be expressed the anode reaction is (M/nanostructure ↔ $M^+ + e^-$) and cathode reaction is ($M^+ + e^- \leftrightarrow$ M). The complete reaction for the LIBs, NIBs and KIBs can be defined via (M^+ + M/nanostructure ↔ M^+/nanostructure + M + ΔG_{cel1}). Finally, in order to calculate the cell voltage (V_{cell}) the Nernst equation are $V_{cell} = -\Delta G_{cell} / zF$; where F is the Faraday constant (96,500 C/mol) and z is the charge of M^+.[68–70]

3. Results and Discussion

3. 1. C_{38} and $Si_{19}Ge_{19}$ as Anode in Metal-ion Batteries

Peyghan et al.[71] investigated the viability of using a BN nanotube for detection of para-chloroaniline molecule by means of density functional theory calculations. Their results showed that the molecule prefers to be adsorbed on the intrinsic BN nanotube from its N atom, releasing energy of 0.65 eV without significant effect on the electrical conductivity of the tube. Their results showed that Si-doped tube detected its presence because of the drastic increase of the electrical conductivity of the tube. Peyghan et al.[72] investigated the adsorption of two anions (F and Cl) and two cations (Li and Na) on the surface of aluminum nitride nanotubes (AlNNTs) by density functional theory. Their results showed that adsorption of anions may facilitate the electron emission from the AlNNT surface by reducing the work function due to the charge transfer occurs from the anions to the tube.

Hosseini et al.[73] investigated the performance of $B_{12}N_{12}$, and its structurally manipulated forms as anode materials for Li-ion batteries (LIBs) by means of density functional theory calculations. Their results shown that encapsulating a fluoride inside the $B_{12}N_{12}$ significantly increased the electrochemical cell voltage (V_{cell}) of $B_{12}N_{12}$.

Najafi et al.[74] examined the applications of $B_{30}N_{30}$, $B_{36}N_{36}$, BNNT (8, 0) and BNNT (10, 0) as anode materials for lithium-ion batteries by density functional theory. Their results shown that V_{cell} of BNNT (8, 0) and BNNT (10, 0) were higher than $B_{30}N_{30}$ and $B_{36}N_{36}$. Their results shown that F functionalization of studied BN-nanostructures improved the potential of anode materials of lithium-ion batteries.

Nejati et al.[75] investigated the potential of $B_{12}N_{12}$ nanocages as anode in Na-ion batteries by density functional theory. Their results shown that encapsulation of different halides ($X = F^-$, Cl^-, Br^-) into BN nanocage increased the cell voltage.

Hosseinian et al.[76] investigated the potential of BN nanosheets in anode of Na-ion batteries by means of density functional theory. Their results shown that replacing three N atoms of the hexagonal ring with larger P atoms increased the performance of the BN nanosheet as an anode of a Na-ion battery but the replacement of B by Al decreased its performance.

Ruiz et al.[77] proven that DFT/M06-2X method can describe the structure and energetics of hybrid inorganic-organic systems with high accuracy. Their results showed that calculated energy error bar values for hybrid inorganic-organic systems correspond to typical experimental error estimates. Their results showed that DFT/M06-2X method has the most accurate results for the binding distance and adsorption energy.

Zhao et al.[78] compared the accuracy and energy error bar of M06-2X functional with 12 other functionals and Hartree Fock theory for 403 energetic data in 29 diverse databases. They recommend M06-2X functional for calculate the thermochemistry, noncovalent interactions and electronic excitation energies to valence and Rydberg states. They suggested the M06-2X functional with high accurate for application in organometallic and inorganometallic chemistry and for noncovalent interactions.

Mahmood et al.[79] examined the performance of 26 combinations of DFT functionals and basis sets were evaluated for the calculation of the activation energy of methylation reactions of nitronates. Their results showed that DFT method and M06-2X functional provided the most accurate results.

Wheeler et al.[80] calculated the enthalpies for bond-forming reactions by using of six DFT functionals and reaction enthalpies were decomposed into contributions from changes in bonding and other intramolecular effects via the hierarchy of homodesmotic reactions. Their results showed that M06-2X has most accurate performance for studied reactions and M06-2X is one of the more accurate functionals for the underlying bond transformations.

Hohenstein et al.[81] showed that M06-2X provide significant improvements over traditional density functionals for the noncovalent interactions. Their results showed that M06-2X correction greatly increases the accuracy of calculations without increasing the computational cost in any significant way. Therefore in previous studies, it can be concluded that DFT/M06-2X method was used for calculation of interactions and energies of various organic and inorganic systems and results showed that DFT/ M06-2X has high accuracy.[77–81]

In this section the potential of C_{38} and $Si_{19}Ge_{19}$ as anodes in LIB, NIB and KIB via DFT method was investigated and novel metal-ion batteries with higher performance were identified. The structures of complexes of C_{38}

Table 1. Calculated G_{ad} (kcal/mol) and bond length (Å) values of studied complexes.

Complex	G_{ad}	Complex	G_{ad}	Complex	G_{ad}
F-C_{37}	–39.99	Cl-C_{37}	–37.84	Br-C_{37}	–35.70
F-$Si_{18}Ge_{19}$	–45.98	Cl-$Si_{18}Ge_{19}$	–43.52	Br-$Si_{18}Ge_{19}$	–41.06
Complex	**Bond**	**Length**	**Complex**	**Bond**	**Length**
Li-C_{38}	Li------C	2.33	Li-$Si_{19}Ge_{19}$	Li------Si	2.73
Na-C_{38}	Na------C	2.47	Na-$Si_{19}Ge_{19}$	Na------Si	2.86
K-C_{38}	K------C	3.15	K-$Si_{19}Ge_{19}$	K------Si	3.55
Li-F-C_{37}	Li------F	2.13	Li-F-$Si_{18}Ge_{19}$	Li------F	2.16
Na-F-C_{37}	Na------F	2.25	Na-F-$Si_{18}Ge_{19}$	Na------F	2.29
K-F-C_{37}	K------F	2.43	K-F-$Si_{18}Ge_{19}$	K------F	2.43
Li-F-C_{37}	F------C	1.37	Li-F-$Si_{18}Ge_{19}$	F------Ge	1.78
Na-F-C_{37}	F------C	1.34	Na-F-$Si_{18}Ge_{19}$	F------Ge	1.76
K-F-C_{37}	F------C	1.36	K-F-$Si_{18}Ge_{19}$	F------Ge	1.77
Li-Cl-C_{37}	Li------Cl	2.51	Li-Cl-$Si_{18}Ge_{19}$	Li------Cl	2.54
Na-Cl-C_{37}	Na------Cl	2.65	Na-Cl-$Si_{18}Ge_{19}$	Na------Cl	2.65
K-Cl-C_{37}	K------Cl	3.36	K-Cl-$Si_{18}Ge_{19}$	K------Cl	3.34
Li-Cl-C_{37}	Cl------C	1.73	Li-Cl-$Si_{18}Ge_{19}$	Cl------Ge	2.18
Na-Cl-C_{37}	Cl------C	1.77	Na-Cl-$Si_{18}Ge_{19}$	Cl------Ge	2.17
K-Cl-C_{37}	Cl------C	1.75	K-Cl-$Si_{18}Ge_{19}$	Cl------Ge	2.16
Li-Br-C_{37}	Li------Br	2.66	Li-Br-$Si_{18}Ge_{19}$	Li------Br	2.67
Na-Br-C_{37}	Na------Br	2.87	Na-Br-$Si_{18}Ge_{19}$	Na------Br	2.86
K-Br-C_{37}	K------Br	3.47	K-Br-$Si_{18}Ge_{19}$	K------Br	3.89
Li-Br-C_{37}	Br------C	1.93	Li-Br-$Si_{18}Ge_{19}$	Br------Ge	2.34
Na-Br-C_{37}	Br------C	1.92	Na-Br-$Si_{18}Ge_{19}$	Br------Ge	2.32
K-Br-C_{37}	Br------C	1.91	K-Br-$Si_{18}Ge_{19}$	Br------Ge	2.34

and $Si_{19}Ge_{19}$ with Li, Na and K were presented in figure 1. The bond lengths in Å of Li, Na and K with C_{38} and $Si_{19}Ge_{19}$ were reported in table 1.

The calculated values of the Gibes free energy (G_{ad}) in kcal/mol of adsorbed metals and metal ions on surfaces of C_{38} and $Si_{19}Ge_{19}$ were presented in table 2. Results show that, all calculated G_{ad} values were negatives and so the studied adsorption were possible from thermodynamic view point. Results show that G_{ad} value of K-C_{38} is higher than G_{ad} values of Li-C_{38} and Na-C_{38}. Also G_{ad} value of K-$Si_{19}Ge_{19}$ is higher than G_{ad} values of Na-$Si_{19}Ge_{19}$ and K-$Si_{19}Ge_{19}$. Results show that G_{ad} values of Li, Na and K on $Si_{19}Ge_{19}$ are higher than G_{ad} values on C_{38}.

Results show that, G_{ad} values of metal ions on C_{38} and $Si_{19}Ge_{19}$ are higher than G_{ad} values of metal on C_{38} and $Si_{19}Ge_{19}$ and the G_{ad} values for studied metal and metal ions have same trends. The G_{ad} values of metal-nanostructure complexes were decreased as following: Li-C_{38} < Na-C_{38} < Li-$Si_{19}Ge_{19}$ < K-C_{38} < Na-$Si_{19}Ge_{19}$ < K-$Si_{19}Ge_{19}$ and for metal ion-nanostructure complexes were decreased as following: Li^+-C_{38} < Na^+-C_{38} < Li^+-$Si_{19}Ge_{19}$ < K^+-C_{38} < Na^+-$Si_{19}Ge_{19}$ < K^+-$Si_{19}Ge_{19}$. So it can be concluded that K or K^+-$Si_{19}Ge_{19}$ and Li or Li^+-C_{38} have the highest and the lowest G_{ad} absolute values, respectively.

The calculated E_{HOMO}, E_{LUMO} and E_{HLG} values in eV of complexes of Li, Na and K with C_{38} and $Si_{19}Ge_{19}$ were reported in table 3. Results show that, E_{HOMO} value of K-C_{38} is lower than E_{HOMO} values of Li-C_{38} and Na-C_{38}. Also E_{HOMO} value of K-$Si_{19}Ge_{19}$ is lower than E_{HOMO} values of Li-$Si_{19}Ge_{19}$ and Na-$Si_{19}Ge_{19}$. Results display that E_{HOMO} values of Li, Na and K on $Si_{19}Ge_{19}$ are lower than E_{HOMO} values on C_{38}.

Results in table 3 show that, E_{HLG} value of K-C_{38} is lower than E_{HLG} values of Li-C_{38} and Na-C_{38}. Also E_{HLG} value of K-$Si_{19}Ge_{19}$ is lower than E_{HLG} values of Li-$Si_{19}Ge_{19}$ and Na-$Si_{19}Ge_{19}$. Results show that, the E_{HLG} values of studied metal-nanostructures were decreased as following: Li-C_{38} > Na-C_{38} > K-C_{38} > Li-$Si_{19}Ge_{19}$ > Na-$Si_{19}Ge_{19}$ > K-$Si_{19}Ge_{19}$. So it can be concluded that K-$Si_{19}Ge_{19}$ and Li-C_{38} have the lowest and the highest E_{HLG} values, respectively.

Hosseini et al.[73] investigated the E_{HLG} values of $B_{12}N_{12}$ and $H_{12}B_{12}N_{12}$ via B3LYP functional and 6-31G (d) basis set and their results shown that E_{HLG} values of $B_{12}N_{12}$ and $H_{12}B_{12}N_{12}$ were 6.84 and 2.51 eV, respectively. Also they calculated the E_{HLG} values of complexes of $B_{12}N_{12}$ and $H_{12}B_{12}N_{12}$ with Li atom and their results shown that the E_{HLG} values of Li-$B_{12}N_{12}$ and Li-$H_{12}B_{12}N_{12}$ were 6.10 and 2.38 eV, respectively.

Nejati et al.[75] calculated the E_{HLG} value of $B_{12}N_{12}$ cage via B3LYP functional and 6-31G (d) basis set in GAMESS software and their results shown that E_{HLG} values of $B_{12}N_{12}$ and Na-$B_{12}N_{12}$ were 6.84 and 1.59 eV, respectively. The E_{HLG} values of complexes of F-$B_{12}N_{12}$, Cl-

$B_{12}N_{12}$ and Br-$B_{12}N_{12}$ with Na atom and their results shown that the E_{HLG} values of Na-F-$B_{12}N_{12}$, Na-Cl-$B_{12}N_{12}$ and Na-Br-$B_{12}N_{12}$ were 1.67, 1.65 and 2.01 eV, respectively.

Hosseinian et al.[76] calculated the E_{HLG} values of BN-nanosheets via B3LYP functional and 6-31G (d) basis set and their results shown that E_{HLG} values of BN-nanosheet, Al-BN-nanosheet and P-BN-nanosheet were 5.88, 4.98 and 5.38 eV, respectively. Also they calculated the E_{HLG} values of complexes of nanosheets with Na atom and their results shown that the E_{HLG} values of Na-BN-nanosheet, Na-Al-BN-nanosheet and Na-P-BN-nanosheet were 1.64, 2.09 and 1.17 eV, respectively.

The calculated V_{cell} in V of complexes of Li, Na and K with C_{38} and $Si_{19}Ge_{19}$ were reported in table 2. Results show that, V_{cell} value of K-C_{38} is higher than V_{cell} values of Li-C_{38} and Na-C_{38}. Also V_{cell} value of K-$Si_{19}Ge_{19}$ is higher than V_{cell} values of Li-$Si_{19}Ge_{19}$ and Na-$Si_{19}Ge_{19}$. Results display that V_{cell} values of Li, Na and K on $Si_{19}Ge_{19}$ are higher than V_{cell} values on C_{38}. Results show that, the V_{cell} values of studied complexes were decreased as following: Li-C_{38} < Na-C_{38} < K-C_{38} < Li-$Si_{19}Ge_{19}$ < Na-$Si_{19}Ge_{19}$ < K-$Si_{19}Ge_{19}$. So it can be concluded that K-$Si_{19}Ge_{19}$ and Li-C_{38} have the highest and the lowest V_{cell} values, respectively.

Finally, it can be concluded: (1) the $Si_{19}Ge_{19}$ as anode in metal-ion batteries has higher potential than C_{38} ca 0.18 V (2) the KIB has higher V_{cell} and higher performance than NIB and KIB ca 0.15 and 0.31 V, respectively.

3. 2. Halogen Adoption of C_{38} and $Si_{19}Ge_{19}$

Hosseini et al.[73] calculated the G_{cell} and V_{cell} values of $B_{12}N_{12}$ and F-$B_{12}N_{12}$ as anode electrodes of Li-ion battery. Their results shown that encapsulating a fluoride inside the BN nanocage can be considered as suitable strategy to improvement the performance of BN nanocage as anode electrode of Li-ion batteries.

Nejati et al.[75] calculated the G_{cell} and V_{cell} values of $B_{12}N_{12}$ as anode electrode of Na-ion battery. Their results shown that the G_{cell} values of F-$B_{12}N_{12}$, Cl-$B_{12}N_{12}$ and Br-$B_{12}N_{12}$ were –85.3, –87.9 and –90.5 kcal/mol, respectively.

In this section the effects of F, Cl and Br adoption on performance of C_{38} and $Si_{19}Ge_{19}$ as anodes of metal-ion batteries via DFT method were investigated. The calculated G_{ad} values of F-, Cl- and Br-doped C_{38} and $Si_{19}Ge_{19}$ were presented in table 1. Results show that, all calculated G_{ad} values were negatives and so the adoption of C_{38} and $Si_{19}Ge_{19}$ with F, Cl and Br were possible from thermodynamic view point.

Results show that G_{ad} value of F-C_{37} is higher than G_{ad} values of Cl-C_{37} and Br-C_{37}. Also G_{ad} value of F-$Si_{19}Ge_{19}$ is higher than G_{ad} values of Cl-$Si_{18}Ge_{19}$ and Br-$Si_{18}Ge_{19}$. Results show that, adoption of C_{38} and $Si_{19}Ge_{19}$ with F atom are possible processes from thermodynamic view point and F-C_{37} and F-$Si_{18}Ge_{19}$ can be suitable candidates as anodes of metal-ion batteries.

In this section the potential of F-, Cl- and Br-doped C_{37} and $Si_{18}Ge_{19}$ as anodes in LIB, NIB and KIB via DFT

Table 2. Calculated G_{ad} (kcal/mol) and V_{cell} (V) values of studied complexes.

Complex	G_{ad}	V_{cell}	Complex	G_{ad}	V_{cell}
K-C_{38}	–7.96	1.44	**K-$Si_{19}Ge_{19}$**	–9.16	1.66
Na-C_{38}	–7.11	1.29	**Na-$Si_{19}Ge_{19}$**	–8.18	1.48
Li-C_{38}	–6.35	1.15	**Li-$Si_{19}Ge_{19}$**	–7.30	1.32
K-F-C_{37}	–17.84	3.23	**K-F-$Si_{18}Ge_{19}$**	–20.51	3.71
Na-F-C_{37}	–15.93	2.88	**Na-F-$Si_{18}Ge_{19}$**	–18.31	3.31
Li-F-C_{37}	–14.22	2.57	**Li-F-$Si_{18}Ge_{19}$**	–16.35	2.96
K-Cl-C_{37}	–16.88	3.05	**K-Cl-$Si_{18}Ge_{19}$**	–19.41	3.51
Na-Cl-C_{37}	–15.07	2.73	**Na-Cl-$Si_{18}Ge_{19}$**	–17.33	3.14
Li-Cl-C_{37}	–13.46	2.43	**Li-Cl-$Si_{18}Ge_{19}$**	–15.48	2.80
K-Br-C_{37}	–15.93	2.88	**K-Br-$Si_{18}Ge_{19}$**	–18.31	3.31
Na-Br-C_{37}	–14.22	2.57	**Na-Br-$Si_{18}Ge_{19}$**	–16.35	2.96
Li-Br-C_{37}	–12.70	2.30	**Li-Br-$Si_{18}Ge_{19}$**	–14.60	2.64
K^+-C_{38}	–41.14		**K^+-$Si_{19}Ge_{19}$**	–47.32	
Na^+-C_{38}	–36.73		**Na^+-$Si_{19}Ge_{19}$**	–42.25	
Li^+-C_{38}	–32.80		**Li^+-$Si_{19}Ge_{19}$**	–37.72	
K^+-F-C_{37}	–92.16		**K^+-F-$Si_{18}Ge_{19}$**	–105.98	
Na^+-F-C_{37}	–82.29		**Na^+-F-$Si_{18}Ge_{19}$**	–94.62	
Li^+-F-C_{37}	–73.47		**Li^+-F-$Si_{18}Ge_{19}$**	–84.49	
K^+-Cl-C_{37}	–87.22		**K^+-Cl-$Si_{18}Ge_{19}$**	–100.30	
Na^+-Cl-C_{37}	–77.87		**Na^+-Cl-$Si_{18}Ge_{19}$**	–89.55	
Li^+-Cl-C_{37}	–69.53		**Li^+-Cl-$Si_{18}Ge_{19}$**	–79.97	
K^+-Br-C_{37}	–82.29		**K^+-Br-$Si_{18}Ge_{19}$**	–94.62	
Na^+-Br-C_{37}	–73.47		**Na^+-Br-$Si_{18}Ge_{19}$**	–84.49	
Li^+-Br-C_{37}	–65.60		**Li^+-Br-$Si_{18}Ge_{19}$**	–75.44	

method was investigated. The structures of complexes of halogen-C_{37} and halogen-$Si_{18}Ge_{19}$ with Li, Na and K were presented in figure 1. The bond lengths of Li, Na and K with halogen-C_{37} and halogen-$Si_{18}Ge_{19}$ and also bond lengths of halogen atoms with bordering C or Ge atoms were reported in table 1.

The calculated G_{ad} values of complexes of metals with halogen-C_{37} and halogen-$Si_{18}Ge_{19}$ were presented in table 2. Results show that, all calculated G_{ad} values were negatives and so the studied adsorption were possible from thermodynamic view point. Results show that G_{ad} value of K-halogen-C_{37} are higher than G_{ad} values of Li-halogen-C_{37} and Na-halogen-C_{37}. Also G_{ad} value of K-halogen-$Si_{18}Ge_{19}$ are higher than G_{ad} values of Na-halogen-$Si_{18}Ge_{19}$ and K-halogen-$Si_{18}Ge_{19}$. Results display that G_{ad} values of Li, Na and K on halogen-$Si_{18}Ge_{19}$ are higher than G_{ad} values on halogen-C_{37}.

Results show that G_{ad} values of F-$Si_{18}Ge_{19}$ and F-C_{37} are higher than G_{ad} values of Cl or Br-$Si_{18}Ge_{19}$ and Cl or Br-C_{37}. The G_{ad} values of complexes of metals with halogen-C_{37} and halogen-$Si_{18}Ge_{19}$ were decreased as following: M-Br-C_{37} < M-Cl-C_{37} < M-F-C_{37} < M-Br-$Si_{18}Ge_{19}$ < M-Cl-$Si_{18}Ge_{19}$ < M-F-$Si_{18}Ge_{19}$. So it can be concluded that K-F-$Si_{18}Ge_{19}$ and Li-Br-C_{38} have the highest and the lowest G_{ad} absolute values, respectively.

The calculated E_{HOMO}, E_{LUMO} and E_{HLG} values in eV of complexes of Li, Na and K with halogen-C_{37} and halogen-$Si_{18}Ge_{19}$ were reported in table 3. Results show that, E_{HOMO} value of K-halogen-C_{37} are lower than E_{HOMO} values of Li-halogen-C_{37} and Na-halogen-C_{37}. Also E_{HOMO} value of K-helogen-$Si_{18}Ge_{19}$ are lower than E_{HOMO} values of Li-halogen-$Si_{18}Ge_{19}$ and Na-halogen-$Si_{18}Ge_{19}$. Results display that E_{HOMO} values of Li, Na and K on halogen-$Si_{18}Ge_{19}$ are lower than E_{HOMO} values of halogen-C_{37}.

Results show that, E_{HLG} value of K-halogen-C_{37} are lower than E_{HLG} values of Li-halogen-C_{37} and Na-halogen-C_{37}. Also E_{HLG} value of K-halogen-$Si_{18}Ge_{19}$ are lower than E_{HLG} values of Li-halogen-$Si_{18}Ge_{19}$ and Na-halogen-$Si_{18}Ge_{19}$. Results show that, the E_{HLG} values of studied complexes were decreased as following: Li-halogen-C_{37} < Na-halogen-C_{37} < K-halogen-C_{37} < Li-halogen-$Si_{18}Ge_{19}$ < Na-halogen-$Si_{18}Ge_{19}$ < K-halogen-$Si_{18}Ge_{19}$. So it can be concluded that K-F-$Si_{18}Ge_{19}$ and Li-Br-C_{37} have the lowest and the highest E_{HLG} values, respectively.

The calculated V_{cell} of complexes of Li, Na and K with halogen-C_{37} and halogen-$Si_{18}Ge_{19}$ were reported in table 2. Results show that, V_{cell} value of K-halogen-C_{37} are higher than V_{cell} values of Li-halogen-C_{37} and Na-halogen-C_{37}. Also V_{cell} value of K-halogen-$Si_{18}Ge_{19}$ are higher than V_{cell} values of Li-halogen-$Si_{18}Ge_{19}$ and Na-halogen-$Si_{18}Ge_{19}$. Results display that V_{cell} values of Li, Na and K on halogen-$Si_{18}Ge_{19}$ are higher than V_{cell} values on halogen-C_{37}. Results show that, the V_{cell} values of studied structures were decreased as following: Li-halogen-C_{37} < Na-halogen-C_{37} < K-halogen-C_{37} < Li-halogen-$Si_{18}Ge_{19}$ < Na-halogen-$Si_{18}Ge_{19}$ < K-halogen-$Si_{18}Ge_{19}$. So it can be concluded that K-F-$Si_{18}Ge_{19}$ and Li-Br-C_{37} have the highest and the lowest V_{cell} values, respectively.

Table 3. Calculated V_{cell} (V) values of studied complexes in water.

Complex	V_{cell}	Complex	V_{cell}
K-C_{38}	1.71	**K-$Si_{19}Ge_{19}$**	1.97
Na-C_{38}	1.53	**Na-$Si_{19}Ge_{19}$**	1.75
Li-C_{38}	1.36	**Li-$Si_{19}Ge_{19}$**	1.56
K-F-C_{37}	3.83	**K-F-$Si_{18}Ge_{19}$**	4.39
Na-F-C_{37}	3.41	**Na-F-$Si_{18}Ge_{19}$**	3.92
Li-F-C_{37}	3.04	**Li-F-$Si_{18}Ge_{19}$**	3.51
K-Cl-C_{37}	3.61	**K-Cl-$Si_{18}Ge_{19}$**	4.16
Na-Cl-C_{37}	3.24	**Na-Cl-$Si_{18}Ge_{19}$**	3.72
Li-Cl-C_{37}	2.87	**Li-Cl-$Si_{18}Ge_{19}$**	3.33
K-Br-C_{37}	3.41	**K-Br-$Si_{18}Ge_{19}$**	3.92
Na-Br-C_{37}	3.04	**Na-Br-$Si_{18}Ge_{19}$**	3.51
Li-Br-C_{37}	2.73	**Li-Br-$Si_{18}Ge_{19}$**	3.13

Finally, it can be concluded: (1) the halogen adoption of nanostructures increased the V_{cell} of studied metal-ion batteries ca 1.5-2.2 V; (2) the F-doped metal-ion batteries have higher V_{cell} than Cl- and Br-doped metal-ion batteries 0.3 and 0.6 V, respectively; (3) K-F-$Si_{18}Ge_{19}$ can

Table 3. Calculated E_{HOMO}, E_{LUMO} and E_{HLG} (eV) values of studied complexes.

Complex	E_{HOMO}	E_{LUMO}	E_{HLG}	Complex	E_{HOMO}	E_{LUMO}	E_{HLG}
K-C_{38}	–4.09	–1.15	2.94	**K-$Si_{19}Ge_{19}$**	–3.78	–1.31	2.48
Na-C_{38}	–4.20	–1.03	3.16	**Na-$Si_{19}Ge_{19}$**	–3.88	–1.17	2.72
Li-C_{38}	–4.30	–0.92	3.38	**Li-$Si_{19}Ge_{19}$**	–3.98	–1.04	2.94
K-F-C_{37}	–3.55	–2.58	0.96	**K-F-$Si_{18}Ge_{19}$**	–3.39	–2.78	0.62
Na-F-C_{37}	–3.79	–2.31	1.48	**Na-F-$Si_{18}Ge_{19}$**	–3.50	–2.65	0.85
Li-F-C_{37}	–4.02	–2.05	1.97	**Li-F-$Si_{18}Ge_{19}$**	–3.69	–2.35	1.34
K-Cl-C_{37}	–3.67	–2.44	1.23	**K-Cl-$Si_{18}Ge_{19}$**	–3.47	–2.65	0.82
Na-Cl-C_{37}	–3.90	–2.18	1.72	**Na-Cl-$Si_{18}Ge_{19}$**	–3.59	–2.50	1.09
Li-Cl-C_{37}	–4.11	–1.95	2.17	**Li-Cl-$Si_{18}Ge_{19}$**	–3.78	–2.23	1.54
K-Br-C_{37}	–3.79	–2.31	1.48	**K-Br-$Si_{18}Ge_{19}$**	–3.55	–2.54	1.01
Na-Br-C_{37}	–4.02	–2.05	1.97	**Na-Br-$Si_{18}Ge_{19}$**	–3.69	–2.35	1.34
Li-Br-C_{37}	–4.22	–1.83	2.38	**Li-Br-$Si_{18}Ge_{19}$**	–3.87	–2.10	1.77

be proposed as novel metal-ion batteries with highest performance.

3.3. Solvent Effects on Potential of Studied Metal-ion Batteries

In this section the effects of water as polar solvent on performance of C_{38}, $Si_{19}Ge_{19}$, and their halogen-doped nanostructures as anode electrodes of metal-ion batteries via via DFT/ M06-2X theory, 6-311+G (2d, 2p) basis set and polarized continuum model (PCM) as solvent model were investigated.[56–61] The calculated V_{cell} values of metal-ion batteries with C_{38}, $Si_{19}Ge_{19}$, and their halogen-doped nanostructures as anode electrodes were presented in table 3.

Results show that, V_{cell} value of K-C_{38} is higher than V_{cell} values of Li-C_{38} and Na-C_{38} in water. Results display that V_{cell} values of Li, Na and K on $Si_{19}Ge_{19}$ are higher than V_{cell} values on C_{38} in water. Results show that in water, V_{cell} value of K-halogen-C_{37} are higher than V_{cell} values of Li-halogen-C_{37} and Na-halogen-C_{37}. Also V_{cell} value of K-halogen-$Si_{18}Ge_{19}$ are higher than V_{cell} values of Li-halogen-$Si_{18}Ge_{19}$ and Na-halogen-$Si_{18}Ge_{19}$ in water. Results display that V_{cell} values of Li, Na and K on halogen-$Si_{18}Ge_{19}$ are higher than V_{cell} values on halogen-C_{37} in water. Results show that, V_{cell} values of studied metal-ion batteries in water are higher than gas phase ca 0.46 V.

4. Conclusion

In this study, the potential of C_{38} and $Si_{19}Ge_{19}$ as anode electrode of Li-ion, Na-ion and K-ion batteries via density functional theory was investigated. Also the effects of halogen adoption of C_{38} and $Si_{19}Ge_{19}$ on ability of metal-ion battery were examined. Obtained results in preset paper are: (1) the $Si_{19}Ge_{19}$ as anode in metal-ion batteries has higher potential than C_{38} ca 0.18 V; (2) the KIB has higher V_{cell} and higher performance than NIB and KIB ca 0.15 and 0.31 V, respectively; (3) the halogen adoption increased the V_{cell} of studied metal-ion batteries ca 1.5–2.2 V; (4) the F-doped metal-ion batteries have higher V_{cell} and higher performance than Cl- and Br-doped metal-ion batteries; (5) K-F-$Si_{18}Ge_{19}$ can be proposed as novel metal-ion batteries with high performance; (6) Results show that, V_{cell} values of studied metal-ion batteries in water are higher than gas phase ca 0.46 V.

5. Acknowledgment

Thanks for all teachers.

6. References

1. M. D. Slater, D. Kim, E. Lee, C. S. Johnson, Adv. *Funct. Mater.* **2013**, *23*, 947–958. **DOI:**10.1002/adfm.201200691
2. Z. Parsaee, P. Haratipour, M. Janghorban Lariche, A. Vojood, *Ultrason. Sonochem.* **2018**, *41*, 337–349. DOI:10.1016/j.ultsonch.2017.09.054
3. J. Barker, M. Y. Saidi, J. L. Swoyer, *Electrochem. Solid-State Lett.* **2003**, *6*, 1–4. **DOI:**10.1149/1.1523691
4. D. Er, J. Li, M. Naguib, *ACS Appl. Mater. Interfaces* **2014**, *6*, 11173–11179. **DOI:**10.1021/am501144q
5. Z. Parsaee, P. Haratipour, M. J. Lariche, A. Vojood, *Ultrason. Sonochem.* **2018**, *41*, 337–349. **DOI:**10.1016/j.ultsonch.2017.09.054
6. W. Gao, P. Haratipour, M. R. R. Kahkha, A. Tahvili, *Ultrason. Sonochem.* **2018**, 44, 152–161. **DOI:**10.1016/j.ultsonch.2018.02.020
7. V. Palomares, P. Serras, I. Villaluenga, *Energy Environ. Sci.* **2012**, *5*, 5884–5901. **DOI:**10.1039/c2ee02781j
8. B. J. Landi, M. J. Ganter, C. D. Cress, *Energy Environ. Sci.* **2009**, *2*, 638–643. **DOI:**10.1039/b904116h
9. A. A. Peyghan, *Struct. Chem.* **2012**, *23*, 1567–1572. **DOI:**10.1007/s11224-012-9970-9
10. A. Rahimi, M. Sepehr, M. J. Lariche, M. Mesbah, A. Kasaeipoor, E. H. Malekshah, *Physica E: Low Dimens. Syst. Nanostruct.* **2018**, *97*, 347–362. **DOI:**10.1016/j.physe.2017.12.003
11. O. Baris¸ Malcioglu, S. Erkoc¸ *J. Mol. Graphics Modell.* **2005**, *23*, 367–371. **DOI:**10.1016/j.jmgm.2004.11.002
12. Z. Bagheri, A. A. Peyghan, *Comp. Theor. Chem.* **2013**, *1008*, 20–26. **DOI:**10.1016/j.comptc.2012.12.011
13. N. L. Hadipour, A. Ahmadi Peyghan, *J. Phys. Chem. C* **2015**, *119*, 6398–6404. **DOI:**10.1021/jp513019z
14. A. Khataee, G. Bayat, J. Azamat, *J. Mol. Graphics Modell.* **2017**, *71*, 176–183. **DOI:**10.1016/j.jmgm.2016.11.017
15. A. Afshar, M. Salami Hosseini, E. Behzadfar, *Sci. Iran. Trans. C* **2014**, *21*, 2107–2115.
16. W. An, X. Wu, X. C. Zeng, *J. Phys. Chem. C* **2008**, *112*, 5747–5755. **DOI:**10.1021/jp711105d
17. Z. Mahdavifar, *J. Mol. Graphics Modell.* **2014**, *54*, 32–45. **DOI:**10.1016/j.jmgm.2014.08.006
18. J. Beheshtian, A. Ahmadi Peyghan, *Physica E* **2012**, *44*, 1963–1968. **DOI:**10.1016/j.physe.2012.06.003
19. X. Wu, W. An, X. C. Zeng, *J. Am. Chem. Soc.* **2006**, *128*, 12001–12006 **DOI:**10.1021/ja063653+
20. J. Beheshtian, *Monatshefte für Chemie/Chemical Monthly* **2012**, *143*, 1623–1626.
21. H Guo, N Lu, J Dai, X Wu, XC Zeng, *J. Phys. Chem. C* **2014**, *118*, 14051–14059 **DOI:**10.1021/jp505257g
22. J. Beheshtian, H. Soleymanabadi, *Appl. Surf. Sci.* **2012**, *268*, 436–441. **DOI:**10.1016/j.apsusc.2012.12.119
23. P. Lu, X. Wu, W. Guo, X. C. Zeng, *Phys. Chem. Chem. Phys.* **2012**, *14*, 13035–13040. **DOI:**10.1039/c2cp42181j
24. E. Vessally, S. Soleimani-Amiri, *Appl. Surf. Sci.* **2017**, *396*, 740–745. **DOI:**10.1016/j.apsusc.2016.11.019
25. J. Beheshtian, A. A. Peyghan, Z. Bagheri, *Appl. Surf. Sci.* **2012**, *258*, 8980–8984. **DOI:**10.1016/j.apsusc.2012.05.134
26. Y. Gao, N. Shao, Y. Pei, Z. Chen, X. C. Zeng, *ACS nano* **2011**, *5*, 7818–7829. **DOI:**10.1021/nn201817b
27. A. A. Peyghan, M. Noei, M. B. Tabar, *J. Mol. Model.* **2013**, *19*, 3007–3014. **DOI:**10.1007/s00894-013-1832-x

28. W. Zhou, J. Zhou, J. Shen, C. Ouyang, *J. Phys. Chem. Solids* **2012**, *73*, 245–251. **DOI:**10.1016/j.jpcs.2011.10.035
29. M. Jeong, T. Ahn, H. Nara, T. Momma, *Nano Energy.* **2016**, *28*, 51–62. **DOI:**10.1016/j.nanoen.2016.08.022
30. Q. Jiang, Z. Zhang, S. Yin, Z. Guo, *Appl. Surf. Sci.* **2016**, *379*, 73–82. **DOI:**10.1016/j.apsusc.2016.03.204
31. D. Shao, D. Tang, J. Yang, Y. Li, *J. Power Sources* **2015**, *297*, 344–350. **DOI:**10.1016/j.jpowsour.2015.08.037
32. P. Subalakshmi, A. Sivashanmugam, *J. Alloys Compd.* **2017**, *690*, 523–531. **DOI:**10.1016/j.jallcom.2016.08.157
33. B. Chen, S. Chu, R. Cai, S. Wei, R. Hu, *Comput. Mater. Sci* **2016**, *123*, 44–51. **DOI:**10.1016/j.commatsci.2016.06.007
34. A. A. Peyghan, M. Noei, *J. Mex. Chem. Soc.* **2014**, *58*, 46–51.
35. A. Gurung, R. Naderi, *Electrochim. Acta* **2016**, *211*, 720–725. **DOI:**10.1016/j.electacta.2016.06.065
36. S. W. Lee, N. Yabuuchi, *Nat. Nanotechnol.* **2010**, *5*, 531–537. **DOI:**10.1038/nnano.2010.116
37. M. Li, Y.-J. Liu, J.-x. Zhao, *Appl. Surf. Sci.* **2015**, *345*, 337–343. **DOI:**10.1016/j.apsusc.2015.03.144
38. L. Qie, W. M. Chen, Z. H. Wang, *Adv. Mater.* **2012**, *24*, 2047–2050. **DOI:**10.1002/adma.201104634
39. Z.-S. Wu, W. Ren, L. Xu, F. Li, *ACS Nano* **2011**, *5*, 5463–5471. **DOI:**10.1021/nn2006249
40. Y. Liu, V. I. Artyukhov, M. Liu, *J. Phys. Chem. Lett.* **2013**, *4*, 1737–1742. **DOI:**10.1021/jz400491b
41. R. P. Hardikar, D. Das, S. S. Han, *Phys. Chem. Chem. Phys.* **2014**, *16*, 16502–16508. **DOI:**10.1039/C4CP01412J
42. A. A. Peyghan, M. Noei, S. Yourdkhani, *Superlattices Microstruct.* **2013**, *59*, 115–122. **DOI:**10.1016/j.spmi.2013.04.005
43. X. Ouyang, M. Lei, S. Shi, C. Luo, D. Liu, *J. Alloys Compd.* **2009**, *476*, 462–465. **DOI:**10.1016/j.jallcom.2008.09.028
44. A. A. Peyghan, Z. Bagheri, *Struct. Chem.* **2013**, *24*, 1565–1570. **DOI:**10.1007/s11224-012-0189-6
45. S. Shi, P. Lu, Z. Liu, Y. Qi, L.G. Hector, *J. Am. Chem. Soc.* **2012**, *134*, 15476–15487. **DOI:**10.1021/ja305366r
46. A. A. Peyghan, A. Soltani, A. A. Pahlevani, *Appl. Surf. Sci.* **2013**, *270*, 25–32. **DOI:**10.1016/j.apsusc.2012.12.008
47. S. Shi, C. Ouyang, M. Lei, W. Tang, *J. Power Sources* **2007**, *171*, 908–912. **DOI:**10.1016/j.jpowsour.2007.07.005
48. A. Ahmadi, J. Beheshtian, M. Kamfiroozi, *J. Mol. Model.* **2012**, *18*, 1729–1734. **DOI:**10.1007/s00894-011-1202-5
49. S. Shi, J. Gao, Y. Liu, Y. Zhao, Q. Wu, W. Ju, *Chin. Phys. B* **2015**, *25*, 018212. **DOI:**10.1088/1674-1056/25/1/018212
50. A. Soltani, A. Ahmadi Peyghan, Z. Bagheri, *Physica E* **2013**, *48*, 176–180. **DOI:**10.1016/j.physe.2013.01.007
51. L. Safari, E. Vessally, A. Bekhradnia, L. Edjlali, *Thin Solid Films* **2017**, *623*, 157–163. **DOI:**10.1016/j.tsf.2017.01.006
52. A. A. Peyghan, M. T. Baei, M. Moghimi, *Comp. Theor. Chem.* **2012**, *997*, 63–69. **DOI:**10.1016/j.comptc.2012.07.037
53. D. Golberg, Y. Bando, Y. Huang, *ACS Nano* **2010**, *4*, 2979–2993. **DOI:**10.1021/nn1006495
54. X. Chen, P. Wu, M. Rousseas, D. Okawa, *J. Am. Chem. Soc.* **2009**, *131*, 890–891. **DOI:**10.1021/ja807334b
55. M. Kamfiroozi, Z. Bagheri, *Chin. J. Chem. Phys.* **2012**, *25*, 60–64. **DOI:**10.1088/1674-0068/25/01/60-64
56. Y. Zhao, D. G. Truhlar, *Theor. Chem. Acc.* **2008**, *120*, 215–241. **DOI:**10.1007/s00214-007-0310-x
57. J. Andzelm, C. Kolmel, *J. Chem. Phys.* **1995**, *103*, 9312–9320. **DOI:**10.1063/1.469990
58. L. H. Gan, J. Q. Zhao, *Physica E* **2009**, *41*, 1249–1252. **DOI:**10.1016/j.physe.2009.02.014
59. S. F. Boys, F. Bernardi, *Mol. Phys.* **1970**, *19*, 553–566. **DOI:**10.1080/00268977000101561
60. L. Ma, J. M. Zhang, K. W. Xu, V. Ji, *Appl. Surf. Sci.* **2015**, *343*, 121–127. **DOI:**10.1016/j.apsusc.2015.03.068
61. J. Beheshtian, H. Soleymanabadi, *J. Mol. Model.* **2012**, *18*, 2343–2348. **DOI:**10.1007/s00894-011-1256-4
62. Z. Bagheri, M. Kamfiroozi, *Struct. Chem.* **2012**, *23*, 653–657. **DOI:**10.1007/s11224-011-9911-z
63. A. A. Peyghan, Z. Bagheri, *Comput. Mater. Sci.* **2012,** *62*, 71–74. **DOI:**10.1016/j.commatsci.2012.05.041
64. R. R. Q. Freitas, G. K. Gueorguiev, *Chem. Phys. Lett.* **2013**, *583*, 119–124. **DOI:**10.1016/j.cplett.2013.07.077
65. M. T. Baei, A. A. Peyghan, Z. Bagheri, *Chin. Chem. Lett.* **2012**, *23*, 965–968. **DOI:**10.1016/j.cclet.2012.06.027
66. M. Baei, H. Mohammadian, *Bulg. Chem. Commun* **2014**, *46*, 735–742.
67. J. Beheshtian, Z. Bagheri, M. Kamfiroozi, *J. Mol. Model.* **2011**, *42*, 1400–1403.
68. J. Beheshtian, Z. Bagheri, M. Kamfiroozi, *J. Mol. Model.* **2012**, *18*, 2653–2658. **DOI:**10.1007/s00894-011-1286-y
69. J. Hosseini, A. Rastgou, R. Moradi, *J. Mol. Liq.* **2017**, *225*, 913–918. **DOI:**10.1016/j.molliq.2016.11.025
70. L. Saw, Y. Ye, A. Tay, *Appl. Therm. Eng.* **2014**, *73*, 154–161. **DOI:**10.1016/j.applthermaleng.2014.06.061
71. M. Eslami, V. Vahabi, A. A. Peyghan, *Physica E,* **2016**,*76,* 6–11. **DOI:**10.1016/j.physe.2015.09.043
72. M. Samadizadeh, S. F. Rastegar, A. A. Peyghan, *Physica E*, **2015**, *69*, 75–80. **DOI:**10.1016/j.physe.2015.01.021
73. J. Hosseini, A. Rastgou, R. Moradi, *J. Mol. Liq.* **2017**, *225*, 913–918. **DOI:**10.1016/j.molliq.2016.11.025
74. M. Najafi M, *Can. J. Chem.* **2017**, *95*. 687–690. **DOI:**10.1139/cjc-2017-0070
75. K. Nejati, A. Hosseinian, A. Bekhradnia, E. Vessally, *J. Mol. Graph. Mod.* **2017**, *74*, 1–7. **DOI:**10.1016/j.jmgm.2017.03.001
76. A. Hosseinian, S. Soleimani, S. Arshadi, E. Vessally, *Phys. Lett. A* **2017**, *381*, 2010–2015. **DOI:**10.1016/j.physleta.2017.04.022
77. T. H. Dunning, *J. Phys. Chem. A* **2000**, *104*, 9062–9065. **DOI:**10.1021/jp001507z
78. V. G. Ruiz, W. Liu, E. Zojer, A. Tkatchenko, *Phys. Rev. Lett.* **2012**, *108*, 146103–146107. **DOI:**10.1103/PhysRevLett.108.146103
79. Y. Zhao, D. G. Truhlar, *Theor. Chem. Account* **2008**, *120*, 215–218. **DOI:**10.1007/s00214-007-0310-x
80. A. Mahmood, R. L. Longo, *Phys. Chem. Chem. Phys.* **2014**, *87*, 1–7.
81. S. E. Wheeler, A. Moran, S. Pieniazek, K. Houk, *J. Phys. Chem. A* **2009**, *113*, 10376–10381. **DOI:**10.1021/jp9058565
82. E. G. Hohenstein, S. T. Chill, C. D. Sherrill, *J. Chem. Theory Comput.* **2008**, *4*, 1996–22001. **DOI:**10.1021/ct800308k

Povzetek

S teoretičnimi raziskavami na podlagi teorije gostotnega potenciala (DFT) smo preučevali C_{38} in $Si_{19}Ge_{19}$ kot materiala, ki bi lahko bila primerena za anode v litij-ionskih, natrij-ionskih in kalij-ionskih baterijah. Dobljeni rezultati so pokazali, da ima $Si_{19}Ge_{19}$ kot anoda v baterijah za približno 0.18 V višji potencial kot C_{38}. Rezultati kalulacij tudi kažejo, da ima kalij-ionska baterija višjo napetost celice kot litij-ionska baterija (približno 0,15 V) in kaliji-ionska baterija (približno 0,31 V). Dodatek halogena naj bi povečal napetost celice v primerih preučevanih baterij za 1,5 do 2,2 V. Izračunana napetost celice v preučevanih sistemih je za približno 0,46 V višja v vodnem mediju kot v plinski fazi. Glede na rezultate kalkulacij v tem sistemu lahko zaključimo, da dodatek fluora v nanokletke $Si_{18}Ge_{19}$ v kalij-ionskih baterijah najbolj izboljša lastnosti baterije in bi ga lahko predlagali kot nov material na tem področju.